A combined approach to cliff characterization: Cliff Stability Index

Rafael J. Bergillos[a,*], Cristobal Rodriguez-Delgado[b,c], Luis Medina[d], Jesús Fernández-Ruiz[d], Jose M. Rodriguez-Ortiz[e], Gregorio Iglesias[f,b]

[a] *Research Institute of Water and Environmental Engineering (IIAMA), Universitat Politècnica de València, Camino de Vera s/n, 46022 Valencia, Spain*
[b] *School of Engineering, University of Plymouth, Plymouth PL4 8AA, UK*
[c] *PROES Consultores, Calle San Germán 39, 28020 Madrid, Spain*
[d] *Department of Geotechnical Engineering, School of Civil Engineering, University of A Coruña, Elviña Campus, 15071 A Coruña, Spain*
[e] *Department of Geotechnical Engineering, School of Architecture, Polytechnic University of Madrid, Avenida Juan Herrera 4, 28040 Madrid*
[f] *MaREI, Environmental Research Institute & School of Engineering, University College Cork, Cork, Ireland*

Abstract

In this work, a combined multidisciplinary method to characterize coastal cliff environments is presented. It combined two complementary approaches – engineering and geomorphological. The first one is represented by the wave power values along the cliff face. For that purpose, the deep-water wave climate is statistically characterized, and high-energy sea states are numerically propagated to the cliff with a state-of-the-art model. The variations in wave power at the cliff face are controlled by the varying cliff orientation and by the irregular morphology, which influences wave propagation through refraction and shoaling processes. Based on wave power, four engineering exposure levels, from low to extreme, are defined and mapped onto the cliff. The geomorphological approach is based on an index developed *ad hoc* for this work, the Cliff Stability (CS) index, which takes into account the cliff geometry, lithology, structure and degradation state, as well as the hydrological conditions. Based on the CS index, four geomorphological exposure levels are defined and mapped, from low to extreme. The combined approach is shown through the application to a study

*Corresponding author.
R.J. Bergillos (E-mail address: rbermec@upv.es)

site in NW Spain. The two perspectives, engineering and geomorphological, are found to yield similar results in some sections of the study area, but not all. It may be inferred that, despite the importance of wave action in shaping the cliff, the additional elements included in the CS index also play a significant role. In practical terms, the significance of these results is that the two approaches, engineering and geomorphological, should be combined to properly characterize coastal cliffs. This combined approach represents a multidisciplinary tool to define and characterize the exposure levels and, thus, prevent damages in cliff environments across the world.

Keywords: Coastal geology; coastal geomorphology; cliff stability; wave power; exposure.

1. Introduction

Coastal cliffs are the most frequent common coastal landforms, representing about 75% of the coastlines around the world (Emery and Kuhn, 1982; Bird, 2011). Some of these cliff coasts represent geological heritage with a great tourist value (Fig. 1), such as the Twelve Apostles (Australia), the Minamijima Island (Japan), the Pigeon Rocks (Lebanon), the Catedral (Peru), the Darwin Arch (Ecuador), the Portada (Chile), the Arco de Cabo San Lucas (Mexico), the Holei Sea Arch and Sunsent Cliffs (United States), the Perce Rock (Canada), the Hvitserkur (Iceland), the Cliffs of Moher (Republic of Ireland), the Arch Rock in Arnarstap (Ireland), the Stacks of Duncansby, Yesnaby and Thirle Door (Scotland), the Green Bridge (Wales), the Durdle Door, Flamborough Head and Old Harry Rocks (England), the Azure Window (Malta), the Drangarnir (Faroe Islands), the Porte d'Aval (France), the Quebrada coast, Cuevas del Mar beach and Cathedral beach (Spain), or the Ponte da Piedade (Portugal), among others.

Figure 1: From left to right, top to bottom: Azure Window, Arco de Cabo San Lucas, Ponte da Piedade, Minamijima Island (first row); Durdle Door, Perce Rock, Arch Rock, Cuevas del Mar (second row); Portada, Porte d'Aval, Moher Cliffs, Quebrada coast (third row); Twelve Apostles, Pigeon Rocks, Green Bridge, Yesnaby (fourth row); Flamborough Head, Thirle Door, Holei Sea Arch, Hvitserkur (fifth row).

Numerous works have studied erosion problems on cliff coasts over the last decades (Sunamura, 1977; Robinson, 1977; Jones and Williams, 1991; Komar and Shih, 1993; Shih and Komar, 1994; Duperret et al., 2002; Moore and Griggs, 2002; Sallenger Jr et al., 2002; Rosser et al., 2005; Hansom et al., 2008; Dawson et al., 2009; Hapke and Plant, 2010; Lim et al., 2011; De Rose and Basher, 2011; Barlow et al., 2012; Dickson et al., 2013; Carpenter et al., 2014; Jones et al., 2015; Johnstone et al., 2016; del Río et al., 2016; Pappalardo et al., 2017; Earlie et al., 2018; Prémaillon et al., 2018; Westoby et al., 2018; Terefenko et al., 2018, 2019; Zelaya Wziatek et al., 2019; Alessio and Keller, 2020; Muñoz-López et al., 2020; Di Crescenzo et al., 2021). For example, Sunamura (1977) proposed, based on field and laboratory data, a relationship between the wave force and the resulting cliff erosion. Later, Jones and Williams (1991) analysed the factors that induce cliff erosion on the Welsh coast through modelling of wave refraction, measurements of annual recession and regression approach. Cliff erosion was also studied during the 90s by means of local controls (Komar and Shih, 1993) and field measurements along the Oregon coast (Shih and Komar, 1994).

In the first decade of this century, Duperret et al. (2002) analysed the collapse of a cliff through stratigraphical dating along with observations and field measurements in France; Rosser et al. (2005) used terrestrial laser scanning to measure and characterize cliff processes in the UK; Dawson et al. (2009) investigated the effects of sediments detached from cliff erosion in the protection of low-lying coastal areas against flooding; and Ogawa et al. (2011) described wave transformation processes across a shore platform based on a field experiment conducted in New Zealand. Other works on cliff erosion over the last ten years have been based on the implementation of models to simulate the erosion of cliffs (Hapke and Plant, 2010; Barlow et al., 2012; Terefenko et al., 2019; Muñoz-López et al., 2020); the study of aerial photographs (De Rose and Basher, 2011; del Río et al., 2016), multiview stereos (Westoby et al., 2018), videos with high resolution (Thompson et al., 2019), and terrestrial and aerial vehicle photometry (Letortu et al., 2018); and the analysis of laser scanning measurements (Lim et al., 2011; De Rose and Basher, 2011; Johnstone et al., 2016; Earlie et al., 2018; Westoby et al., 2018; Terefenko et al., 2018, 2019; Zelaya Wziatek et al., 2019; Alessio and Keller, 2020).

This work proposes a novel method to characterize coastal cliff environments, which combines geomorphological and engineering approaches. The combined approach is used to characterize a study site in north-western Iberian Peninsula. The engineering approach, which is represented by the wave power impinging on the cliff, covers the statistical analysis of deep-water wave climate, the numerical wave propagation toward the cliff of relevant sea states, and the assessment of wave power values on the cliff face. The geomorphological approach is based on a novel index, defined *ad hoc*: the Cliff Stability (CS) index, including the characterization of the cliff geometry, lithology, structure, degradation state and hydrological conditions.

2. Study site

The Catedrales cliff and beach are located in the Atlantic Ocean littoral of northwest Spain, in the Iberian Peninsula (Figs. 2 and 3). The stretch of coastline considered in this study has a length of 1700 m. This area, of great environmental and tourism value, was registered as Natural Monument in 2005.

Figure 2: (a) Study site location (north-western Iberian Peninsula). (b) Plan view of the Catedrales cliff and beach.

The Catedrales beach is located to the West of the basal thrust of the Manto de Mondoñedo and more specifically between the Eo anticline and the Villaodrid syncline. The rocks of the Catedrales beach belong to the Los Cabos

Figure 3: Catedrales Cliffs.

formation, and in particular to the Brens layer (Bastida and Pulgar, 1978). The stratigraphic profiles present on the cliffs are formed by levels of sandstone with insertions of siltstone layers, under which a harder and more resistant series formed by quartzite and gray slate is located, which has somewhat greater thickness and may appear in alternation. These profiles can be affected by other geological structures associated with existing tectonics, such as main or secondary faults, minor folds and shear zones related with sub-horizontal thrust faults.

All along the cliff there are several strongly-inclined-plane faults of unequal relevance, in which two main groups of directions stand out: NNE-SSW and WNW-ESE. The analysis of the existing joint families allows determining the strong tectonic control acting all along the cliff, which has determined the geomorphological units related to the cliff evolution itself. The structural arrangement has conditioned the coastline morphology as well as the appearance of all existing geomorphological units, such as galleries, caves, blowholes, cliffs, stacks, etc.

The wave climate in the study site is highly energetic due to its location, exposed to the long Atlantic fetch (Carballo et al., 2015a,b; Veigas et al., 2015). The mean wave direction is north-west (Fig. 4). Under storm conditions, significant wave heights in deep water exceed ten meters. These storm waves erode the cliff, causing material damages and, tragically, loss of human life. A tourist was killed in March 2018 by a stone falling from the cliff.

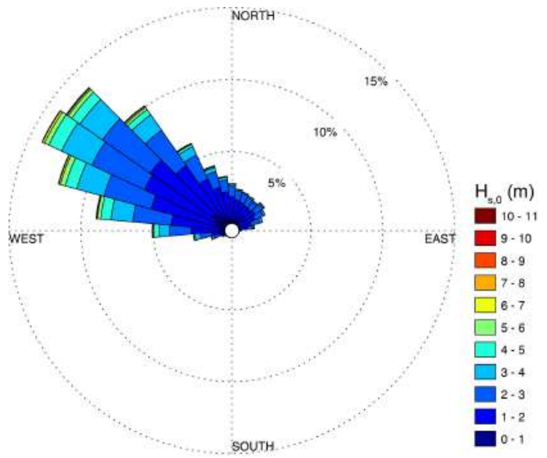

Figure 4: Deep-water wave rose at the study site. Data source: ERA5 model

3. Methods

3.1. Wave data and treatment

3.1.1. Deep-water wave climate

The Peak Over Threshold (POT) method (Goda, 2010) was used to statistically characterise the extreme regime of deep-water significant wave heights. For this purpose, the data series of the ERA5 model of the ECMWF (European Centre for Medium-Range Weather Forecast) were employed. To apply the POT method, a threshold value equal to the significant wave height that is exceeded 1% of the time (i.e., $H_T = H_{99\%}$) was considered. After the Peak Over Threshold method was applied, several theoretical cumulative distribution functions were fitted to selected extreme significant wave height values.

3.1.2. Numerical wave propagation

The wave propagation model *SWAN* (Holthuijsen et al., 1993; Booij et al., 1999) was used to propagate the sea states detailed in the previous section under high-tide conditions, from deep water (ERA5 node location, Fig. 5) towards the cliff toe. This numerical wave propagation model has been used for a wide range of coastal engineering applications in the past few years (Bergillos et al., 2016a; López-Ruiz et al., 2016a; Bergillos et al., 2016b, 2017b,a; López-Ruiz et al., 2016b; Bergillos et al., 2018b,a; Magaña et al., 2018; López-Ruiz et al., 2018b,a; Rodriguez-Delgado et al., 2018a,b, 2019b; Bergillos et al., 2019c,a,b; Rodriguez-Delgado et al., 2019c,a, 2020; Rodriguez-Delgado and Bergillos, 2021).

To set up and apply the wave propagation model, bathymetric and topographic data collected over a field campaign were used. The bathymetric measurements were complemented by bathymetric data of the European Marine Observation and Data network, EMODnet (Thierry et al., 2019). Two numerical grids were also defined and employed (Fig. 5): a coarse grid along the whole numerical domain and a nested grid located only at the nearshore zone, with a lower plan view area but a greater resolution.

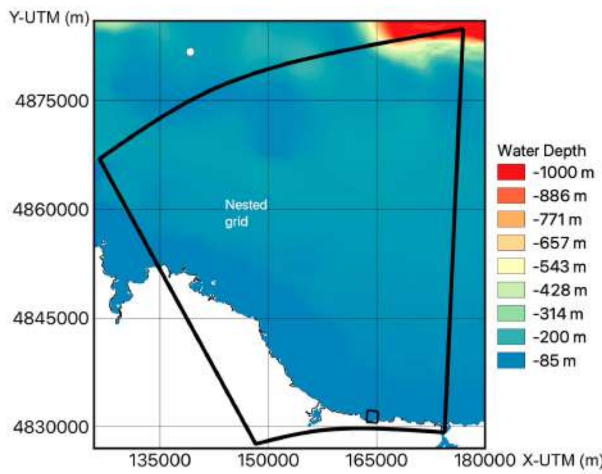

Figure 5: Water depths (in m), computational grids used for the *SWAN* numerical model, and ERA5 point location.

3.1.3. *Wave power acting on the cliff face*

The results obtained with *SWAN* were used to compute wave power through the equation (Astariz and Iglesias, 2016a,b):

$$P = \frac{1}{16}\rho g H_s^2 C_g \,, \tag{1}$$

where g is acceleration of gravity, H_s is significant wave height, ρ is density of water, and C_g is celerity of the wave group, computed as (Besio et al., 2016; Contestabile et al., 2017):

$$C_g = \frac{c}{2}\left(1 + \frac{2kh}{\sinh(2kh)}\right)\sqrt{\frac{g}{h}\,\tanh(kh)}\,, \tag{2}$$

where h is water depth, c is wave celerity, and k is wave number.

3.1.4. Definition and mapping of exposure levels

The following exposure levels were defined according to the engineering approach:

- Low exposure (LE): Wave power < 4.6 kW/m,
- Middle exposure (ME): $4.6 \leq$ Wave power < 9.2 kW/m,
- High exposure (HE): $9.2 \leq$ Wave power < 13.8 kW/m,
- Extreme exposure (EE): Wave power ≥ 13.8 kW/m.

These exposure levels were mapped along the study area.

3.2. Geomorphological approach and Cliff Stability (CS) index

The geomorphological approach was based on the novel Cliff Stability (CS) index, defined *ad hoc* as the weighted sum of factors relating to the geometry, lithology, structure, degradation state and hydrological conditions of the cliff. Whereas the first four factors (geometry, lithology, structure and degradation state) are related to the properties of the cliff, the hydrological conditions (precipitation, wave action) depend not only on the properties of the cliff (e.g., infiltration, orientation) but also on the cliff location.

The Cliff Stability (CS) index is defined as

$$CS = (G + L + E_1 + E_2 + D) \cdot P \cdot W, \tag{3}$$

where G represents the influence of the geometry, L the lithology, E_1 the macro-structure, E_2 the micro-structure, D the degradation state, P the precipitation and W the wave action.

The maximum value of the CS index was set to 100, by definition. The ranges of the factors in Equation (3) were chosen to represent the influence of each factor on the cliff stability. The maximum values established for P and W were 1.11 and 1.5, respectively. As regards the other factors, the following ranges were considered: G varies between 0 and 4, L between 0 and 14, E_1 between 0 and 8, E_2 between 0 and 16, and D between 0 and 18. Thus, the maximum value of the sum of factors in brackets in Equation (3) is 60. The evaluation of these factors based on the field campaign is explained below. The field campaign was meticulously carried out by two experienced geologists over three months.

The study site was divided into 24 zones with similar characteristics and conditions (Fig. 6). In each zone, the CS index was quantified at the upper and lower parts of the cliff face through *in situ* observations. The CS assigned to each zone is the maximum value of the two obtained for the upper and lower parts.

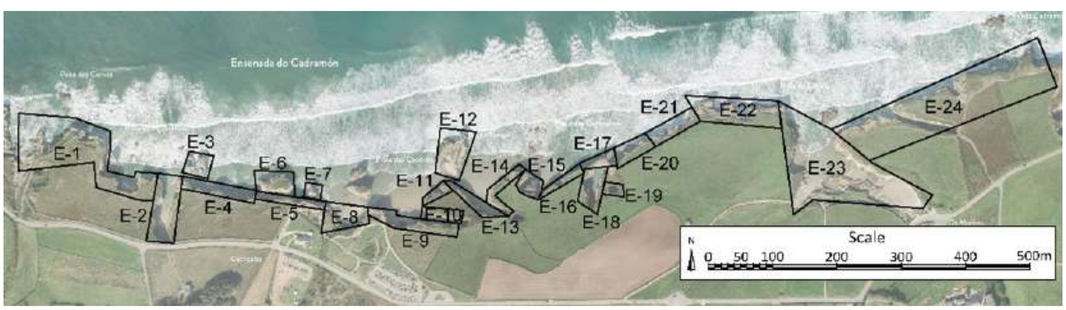

Figure 6: Zonification for the geomorphological approach.

3.2.1. *Geometry*

The geometry factor (G) is obtained based on the height of the cliff and the type of cliff profile (Table 1). Thus, in the stretches with cliff heights below 6 m, G varies between 1 (for vertical cliff profiles or cliff profiles leaning toward the land) and 2 (for cliff profiles leaning toward the sea). For stretches of cliff higher than 6 m and below 12 m, G varies between 1.5 m and 3 m. Finally, for cliffs with heights greater than 12 m, G is between 2 and 4.

Table 1: Values of the geometry factor (G) depending on the height of the cliff (H) and the cliff profile.

Cliff profile	$H \leq 6$ m	$6 < H \leq 12$ m	$H > 12$ m
Vertical or leaning towards the land	1	1.5	2
Leaning towards the sea	1.5	2.5	3
With undermining at the lower part	2	3	4

3.2.2. Lithology

The rocks of the Aguasantas cliff belong to the Los Cabos Formation, and in particular to the Brens layer, where there is an alternation of quartzites, sandstones, siltstones and slates. The lithology factor (L) depends on the rock layer thickness and also on the typology of the rock: hard and abrasion resistant (e.g., quartzites and quartz schists), soft and erodible (e.g., lightly cemented sandstones and phyllites) or mixed (Table 2).

Table 2: Values of the lithology factor (L) as a function of the rock layer thickness (S) and the rock type.

Rock type	$S \leq 0.3$ m	$S > 0.3$ m
Hard and abrasion resistant	6	3
Soft and erodible	14	9
Mixed	10	6

3.2.3. Structure

Two types of structure factors are considered: macro-structure (E_1, Table 3), like large cracks or open vertical joints, and micro-structure (E_2, Table 4), which takes into account the number of discontinuities and the type of discontinuities that weaken the rock mass (apart from those considered by E_1).

Table 3: Values of the macro-structure factor (E_1) as a function of the main stratification.

Main stratification	$E1$
Subvertical and parallel to the slope	8
Subvertical and perpendicular to the slope	2
Subhorizontal	6
Oblique with variable inclination	4

Table 4: Values of the micro-structure factor (E_2) as a function of the type of joints (smooth, rough or filled) and the frequency of the joints.

Frequency of the joints	Smooth joints	Rough joints	Filled joints
Low frequency	6-10	4-6	6-8
Middle frequency	8-12	6-8	8-10
High frequency	10-16	8-12	9-14

3.2.4. Degradation state

The degradation factor (D) was obtained through the characterization of several significant phenomena observed: the rockfalls, cornices at the top of the cliffs, opened cracks, relevant landslides, the volume of caves and the temporal evolution of the fauna and flora attached to the cliff (which is indicative of the temporal evolution of the degradation), as it is indicated in Table 5.

Table 5: Values of the degradation state factor (D) as a function of the degree of degradation, temporal evolution, rockfalls volume, frequency of cornices and volume of caves.

Degree of degradation	Temporal evolution	Volume of rockfalls			Frequency of cornices			Volume of caves		
		High	Middle	Low	High	Middle	Low	High	Middle	Low
	Insignificant	6	4	2	6	4	2	8	6	4
Null or light	Short term	10	8	6	10	8	6	12	10	8
	Long term	8	6	4	8	6	4	10	8	6
	Insignificant	10	8	6	10	8	6	12	10	8
Middle	Short term	14	12	10	14	12	10	16	14	12
	Long term	12	10	8	12	10	8	14	12	10
	Insignificant	12	10	8	12	10	8	14	12	10
High	Short term	16	14	12	16	14	12	18	16	14
	Long term	14	12	10	14	12	10	16	14	12

3.2.5. Hydrological conditions

Two hydrological conditions are considered to assess the CS index: precipitation and wave power. The assessment of the effects of the water on the cliff was performed after an intense rain. The value of the precipitation factor (P) depends on the runoff from the crowning of the cliff, and the presence or absence of corrective actions, such as sealing layers (Table 6).

Table 6: Values of the precipitation factor (P) as a function of the runoff from the crowning of the cliff and the corrective actions.

Runoff	With corrective actions	Without corrective actions
Null	1	1
Middle	1	1.05
Important	1.05	1.11

The wave power factor (W) was quantified based on the wave exposure levels obtained with the engineering approach and the type of sediment (sand or gravel), as it is indicated in Table 7.

Table 7: Values of the wave power factor (W) as a function of the sediment type at the cliff toe and the wave exposure (low, middle, high or extreme).

Sediment type	Low exp.	Middle exp.	High exp.	Extreme exp.
Sand	1	1.1	1.2	1.3
Gravel	1	1.2	1.35	1.5

3.2.6. Geomorphological mapping of exposure levels

The exposure levels in the geomorphological approach were established on the basis of the CS index defined by Eq. (3). Four geomorphological exposure levels were established (Table 8) and these levels were mapped along the study site.

Table 8: Geomorphological exposure levels as a function of the CS index values.

Exposure level	CS range
Low exposure	$CS < 25$
Middle exposure	$25 < CS < 50$
High exposure	$50 < CS < 75$
Extreme exposure	$CS > 75$

4. Results

Among the theoretical cumulative distribution functions (CDF) tested, the best fit to the extreme significant wave height values was obtained with by the Generalized Extreme Value function. Based on this Generalized Extreme Value CDF, the values of wave height for return periods of 2 years, 10 years, 50 years and 100 years were calculated to be 6.6 m, 8.3 m, 11 m and 12.7 m, respectively (Fig. 7).

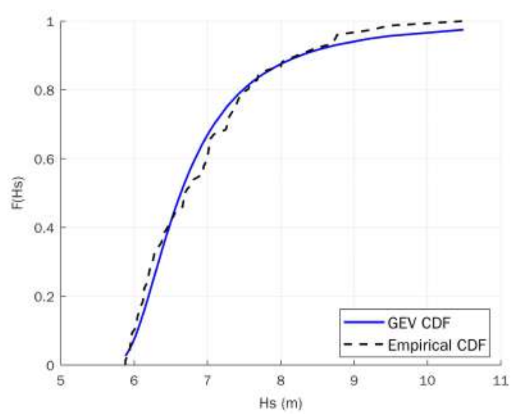

Figure 7: Generalised Extreme Value function and empirical CDF of the significant wave height values (H_s) above the threshold.

These significant wave heights in deep water, the most typical peak period under storm conditions and the most frequent incoming mean direction under high-energy conditions (T_p=15 s and θ=300°) were numerically propagated toward the cliff toe for high-tide conditions by means of the $SWAN$ model, presented in Section 3.1.2. Fig. 8 shows the significant wave heights within the nested grid for the four return periods considered: 2 years, 10 years, 50 years and 100 years. Deep-water significant wave heights range from 3.3 m to 5.5 m, for return periods of 2 and 100 years, respectively. This dependence of the significant wave height upon the return period occurs in deep and transitional water but not in the shallow water in front of the cliff due to wave breaking induced by depth (Fig. 6). In the shallow water nearshore there is some variation in the wave height values at the cliff face. This is induced by wave refraction and shoaling due to the irregular bathymetry. In particular, close to the west boundary of the nested grid, the lower water depths lead to wave breaking at longer distances from the cliff toe, resulting in an area of lower significant wave heights.

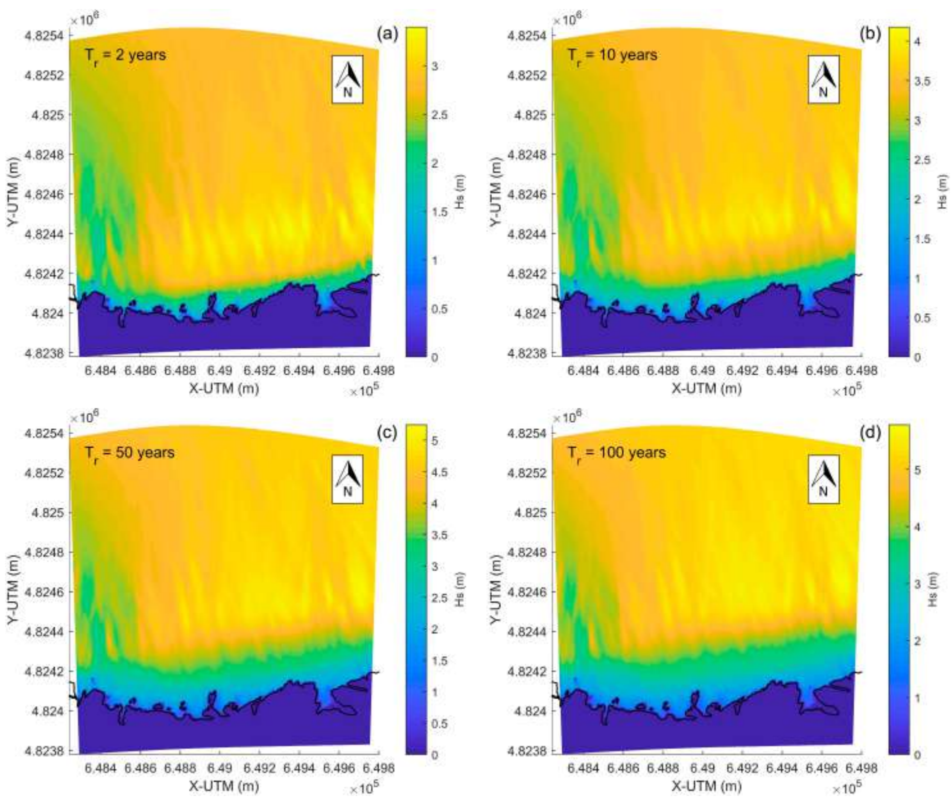

Figure 8: Significant wave height distributions in the nested grid for return periods of 2, 10, 50 and 100 years.

The values of wave power on the cliff face were quantified for the deep-water significant wave height value corresponding to a return period of 2 years (i.e., $H_{s,0}$ =6.6 m) given that, as reported in the previous paragraph, the wave height values at the cliff face do not vary for the different return periods (Fig. 8). Fig. 9a shows the wave power distribution in the nested grid. The wave breaking induced by water depth reduces the wave power at the cliff face. In the western part of the nested grid the lower water depths reduce the significant wave heights in that area (Fig. 8) and, therefore, the wave power (Fig. 9a).

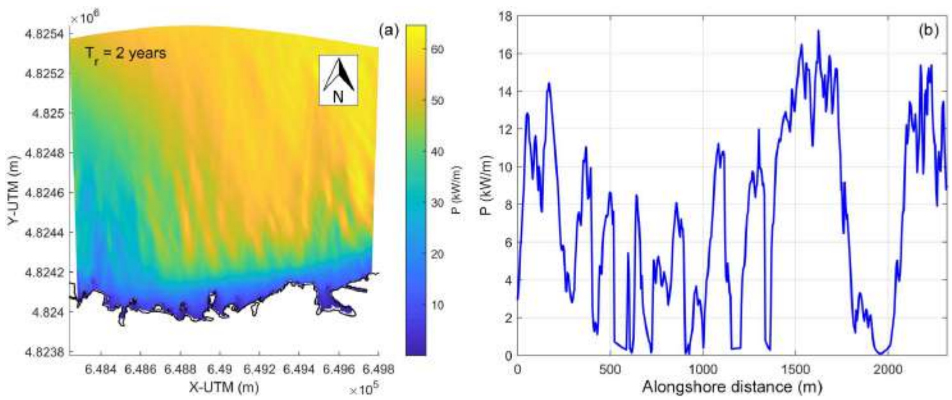

Figure 9: Wave power distribution in the nested grid (a) and variability of wave power values along the cliff face (b) for a 2-year return period.

The right panel of Fig. 9 presents the distribution of wave power values at the cliff toe. This distribution is highly variable due to the variation in significant wave heights at the cliff face, which is induced, in turn, by the different cliff orientations and complex bathymetry of the study site. The irregular wave power distribution on the cliff leads to different levels of cliff exposure from the engineering point of view.

The mapping of the exposure levels obtained with the engineering approach along the study site is shown in Fig. 10. It may be observed that exposure levels are ultimately controlled by the cliff orientation and the nearshore bathymetry, which influences the variations in significant wave heights (and other wave properties) in the propagation from deep water toward the cliff and the resulting wave power distribution at the cliff face. These wave power variations lead to the different exposure levels from the engineering point of view (Fig. 10). For instance, the inlet close to the east boundary of the study site is a LE zone since the wave power values in this area (Fig. 9b, $s \approx 2000$ m) are low.

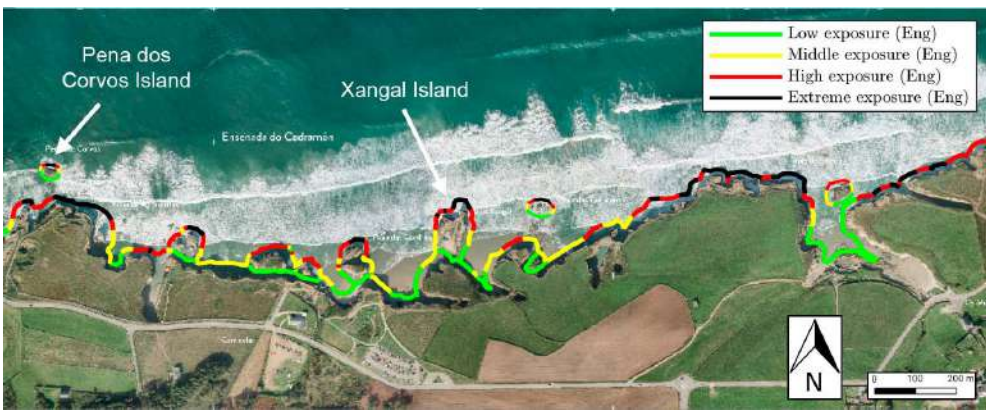

Figure 10: Exposure levels according to the engineering approach.

The Pena dos Corvos Island (west zone of the study site; Fig. 10) has HE and EE levels on its north face and LE level on its south face due to the protection provided by the island and the higher water depths on the north face. The Xangal Island (central zone of the study site; Fig. 7) leads to a similar exposure variability, with HE and EE levels in the windward face and a LE level in the leeward face. In the study area there are also some isolated rocks near the cliff face, which act as submerged (emerged) marine structures for high (low) astronomical tides, reducing the wave power values impinging on the cliff. This mitigation of wave power is, obviously, less effective than that provided by the aforementioned islets.

On the other hand, based on the exposure levels obtained by means of the geomorphological approach (Fig. 11), the exposure of the cliffs located in the western zone of the study site is high. This high exposure is extended until the central stretch of beach, with only a small zone of middle exposure in the eastern part of the inlet (zone E-2, Fig. 6). In the central stretch of beach the level of exposure is generally low or middle, whereas in the Xangal Islet the exposure is high. From this section of beach toward the eastern boundary, the exposure is middle to high, except a small section of low exposure at the eastern inlet (zone E-23, Fig. 6).

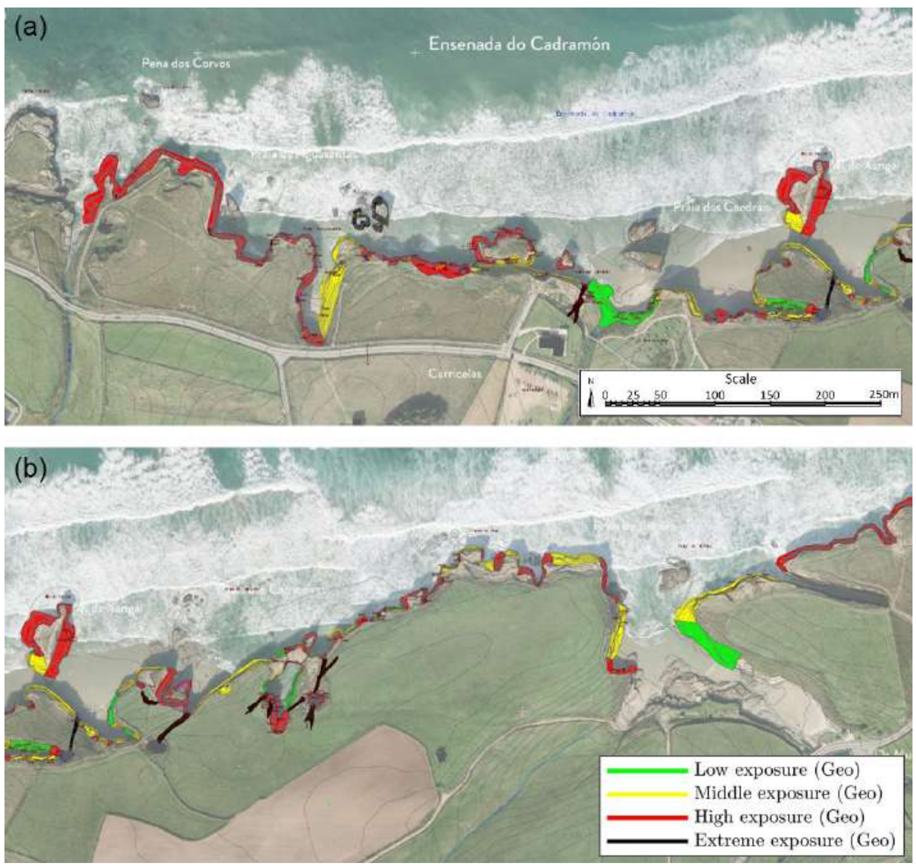

Figure 11: Exposure levels according to the geomorphological approach: (a) From zone E-1 to zone E-13, (b) from zone E-14 to zone E-24.

5. Discussion

A previous approach to the problem addressed in this work was made by Gornitz et al. (1991), who proposed the first Coastal Vulnerability Index (CVI), composed of seven variables as indicators of physical vulnerability due to the see level rise. These variables consisted of relief (elevation), lithology, geomorphology, erosion/accretion, tidal range, wave height, and relative sea-level changes. This methodology was improved later by Gornitz et al. (1994), who added new variables as permanent inundation (elevation and local subsidence) and episodic inundation (tropical storm probability, hurricane probability, hurricane frequency-intensity, etc.). However, this approach was mainly oriented to the assessment of coastal vulnerability due to future sea level rise from greenhouse climate warming. Conversely, the CS index presented in this paper focuses mainly on the current geological and marine conditions because these cliffs are visited annually by more than 500,000 people and it is necessary to estimate the current vulnerability of the cliffs. Furthermore, the CS index takes into account some variables which are not included in the CVI and which play a relevant role in the particular case of the Catedrales cliffs: the macro and microstructure of the rock formations, the rainfall and runoff from the crowning of the cliff, the sediment type at the cliff toe, the wave exposure level and the degradation state of the cliffs.

When the results of both approaches (engineering and geomorphological) are compared, a clear parallelism is apparent. There are, of course, some differences, which might have been expected given that both approaches are based on different indicators – wave power and Cliff Stability (CS) index. At any rate, these differences are not greater than one exposure level, excepting four small zones which have been marked and numbered in Fig. 12. In the cases marked as (1), (2) and (4) the geomorphological exposure is higher because of the abundant rockfalls resulting from erosive phenomena of non-marine origin. By contrast, in the case marked as (3) the engineering exposure is greater because the lithology corresponds to a homogeneous profile formed by the hardest and more resistant rocks in the zone, such as quartzites and quartz schists.

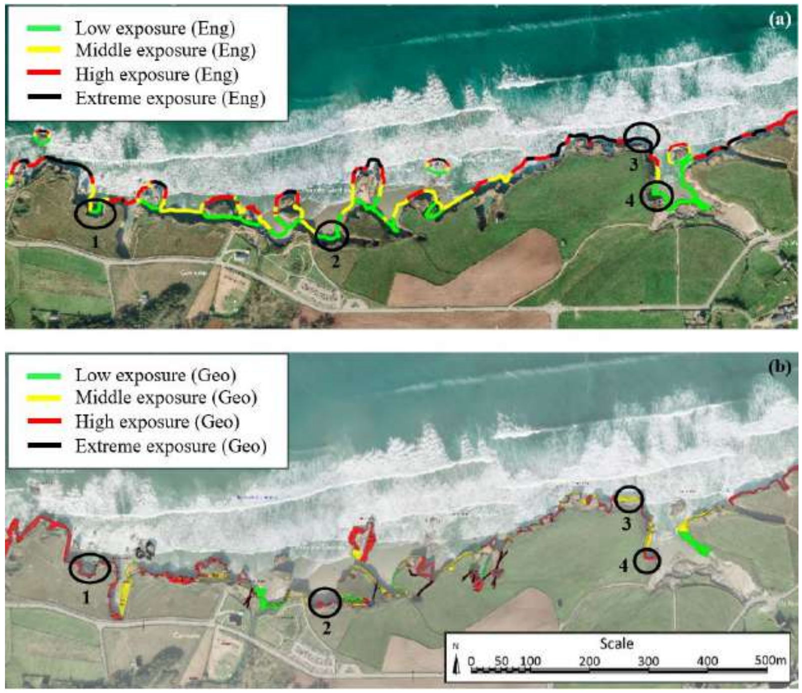

Figure 12: Comparison of exposure levels based on engineering (a) and geomorphological (b) approaches.

6. Conclusions

This work proposes a multidisciplinary approach for the characterization of coastal cliffs based on engineering and geomorphological points of view. The combined approach was applied to a study site in northwest Spain.

The engineering approach was characterized through wave power values along the cliff toe, which were obtained by combining statistical approach and wave propagation modelling. The results of the engineering approach reveal the high variability in the wave power values along the cliff toe. That irregular distribution stems from: (1) the varying orientation of the shoreline with respect to the prevailing wave direction, so that some cliffs are more exposed than others to the incoming waves, and (2) the complex bathymetry at the nearshore region, which controls wave shoaling and refraction. On the basis of wave power, four exposure levels, from low to extreme, were established and mapped. For instance, the windward faces of the islets in front of the main shoreline present high or extreme exposure levels, whereas the leeward faces of the islets and the inlets along the main shoreline have low exposure levels.

The geomorphological approach was based on the Cliff Stability (CS) index, a new parameter developed *ad hoc* for this work, which may be applied to characterise other cliffs elsewhere. The CS index is a function of the cliff geometry, lithology, structure and degradation state along with the hydrological conditions. For the analysed case study, the CS index is more appropriate than the existing Coastal Vulnerability Index (CVI), since the CVI does not include some variables which play a relevant role in the particular case of the Catedrales cliffs, such as the macro and microstructure of the rock formations, the rainfall and runoff from the crowning of the cliff, the sediment type at the cliff toe, the wave exposure level and the degradation state of the cliffs. The values of the CS index served to define and map four exposure levels (from low to extreme, as in the engineering approach) onto the study area. Most of the study area was categorized as high exposure, except the inlets and the central stretch of beach.

The comparison of both approaches reveals similar results in some zones, such as western boundaries of the study area or the north face of the Xangal Islet. However, differences were observed in other areas, such as the west bank of the inlet near the eastern boundary of the study area or the leeward face of the Xangal Islet. The conclusion that may be drawn from these differences is that wave power is important in shaping the cliff, but the rest of elements contained in the CS index (geometry, lithology, structure, degradation state or precipitation) also play a role. These results highlight the interest of combining the two approaches, engineering and geomorphological, in characterising cliff coasts, and the usefulness of the novel Cliff Stability (CS) index. This combined approach, which is extensible to other coastal cliff environments elsewhere, may be used as a management tool, in particular for the prevention of material and human damages by determining the most exposed zones.

Acknowledgements

This work was carried out in the framework of the project "Study to establish the current geomorphological and geotechnical situation of the natural monument Catedrales beach and its possible evolution in time", which was funded by the *Xunta the Galicia* (Spain) and the European Union. R.B. was partly funded by MCIN/AEI/10.13039/501100011033 through Juan de la Cierva program (research contract IJC2019-038848-I) and C.R.D. was partly funded by the University of Plymouth (United Kingdom). We thank two anonymous reviewers for their suggestions to improve this work.

References

Alessio, P., Keller, E.A., 2020. Short-term patterns and processes of coastal cliff erosion in Santa Barbara, California. Geomorphology 353, 106994.

Astariz, S., Iglesias, G., 2016a. Output power smoothing and reduced downtime period by combined wind and wave energy farms. Energy 97, 69 – 81.

Astariz, S., Iglesias, G., 2016b. Selecting optimum locations for co-located wave and wind energy farms. part ii: A case study. Energy Conversion and Management 122, 599 – 608.

Barlow, J., Lim, M., Rosser, N., Petley, D., Brain, M., Norman, E., Geer, M., 2012. Modeling cliff erosion using negative power law scaling of rockfalls. Geomorphology 139, 416–424.

Bastida, F., Pulgar, J.A., 1978. La estructura del manto de Mondoñedo entre Burela y Tapia de Casariego (Costa Cantábrica, NW de España) .

Bergillos, R.J., Lopez-Ruiz, A., Medina-Lopez, E., Monino, A., Ortega-Sanchez, M., 2018a. The role of wave energy converter farms on coastal protection in eroding deltas, Guadalfeo, southern Spain. Journal of Cleaner Production 171, 356–367.

Bergillos, R.J., López-Ruiz, A., Ortega-Sánchez, M., Masselink, G., Losada, M.A., 2016a. Implications of delta retreat on wave propagation and longshore sediment transport - Guadalfeo case study (southern Spain). Marine Geology 382, 1–16.

Bergillos, R.J., López-Ruiz, A., Principal-Gómez, D., Ortega-Sánchez, M., 2018b. An integrated methodology to forecast the efficiency of nourishment strategies in eroding deltas. Science of the Total Environment 613, 1175–1184.

Bergillos, R.J., Masselink, G., McCall, R.T., Ortega-Sánchez, M., 2016b. Modelling overwash vulnerability along mixed sand-gravel coasts with XBeach-G:

Case study of Playa Granada, southern Spain, in: Coastal Engineering Proceedings, p. 13.

Bergillos, R.J., Masselink, G., Ortega-Sánchez, M., 2017a. Coupling cross-shore and longshore sediment transport to model storm response along a mixed sand-gravel coast under varying wave directions. Coastal Engineering 129, 93–104.

Bergillos, R.J., Rodriguez-Delgado, C., Allen, J., Iglesias, G., 2019a. Wave energy converter configuration in dual wave farms. Ocean Engineering 178, 204–214.

Bergillos, R.J., Rodriguez-Delgado, C., Allen, J., Iglesias, G., 2019b. Wave energy converter geometry for coastal flooding mitigation. Science of the Total Environment 668, 1232–1241.

Bergillos, R.J., Rodriguez-Delgado, C., Iglesias, G., 2019c. Wave farm impacts on coastal flooding under sea-level rise: a case study in southern Spain. Science of the Total Environment 653, 1522–1531.

Bergillos, R.J., Rodríguez-Delgado, C., Ortega-Sánchez, M., 2017b. Advances in management tools for modeling artificial nourishments in mixed beaches. Journal of Marine Systems 172, 1–13.

Besio, G., Mentaschi, L., Mazzino, A., 2016. Wave energy resource assessment in the Mediterranean Sea on the basis of a 35-year hindcast. Energy 94, 50–63.

Bird, E.C., 2011. Coastal geomorphology: an introduction. John Wiley & Sons.

Booij, N., Ris, R.C., Holthuijsen, L.H., 1999. A third-generation wave model for coastal regions: 1. Model description and validation. Journal of geophysical research: Oceans 104, 7649–7666.

Carballo, R., Sánchez, M., Ramos, V., Fraguela, J., Iglesias, G., 2015a. Intra-annual wave resource characterization for energy exploitation: A new decision-aid tool. Energy conversion and management 93, 1–8.

Carballo, R., Sánchez, M., Ramos, V., Fraguela, J., Iglesias, G., 2015b. The intra-annual variability in the performance of wave energy converters: A comparative study in N Galicia (Spain). Energy 82, 138–146.

Carpenter, N., Dickson, M., Walkden, M., Nicholls, R., Powrie, W., 2014. Effects of varied lithology on soft-cliff recession rates. Marine Geology 354, 40–52.

Contestabile, P., Lauro, E.D., Galli, P., Corselli, C., Vicinanza, D., 2017. Offshore wind and wave energy assessment around Malè and Magoodhoo Island (Maldives). Sustainability 9, 613.

Dawson, R.J., Dickson, M.E., Nicholls, R.J., Hall, J.W., Walkden, M.J., Stansby, P.K., Mokrech, M., Richards, J., Zhou, J., Milligan, J., Jordan, A., Pearson, S., Rees, J., Bates, P.D., Koukoulas, S., Watkinson, A.R., 2009. Integrated analysis of risks of coastal flooding and cliff erosion under scenarios of long term change. Climatic Change 95, 249–288.

De Rose, R.C., Basher, L.R., 2011. Measurement of river bank and cliff erosion from sequential LIDAR and historical aerial photography. Geomorphology 126, 132–147.

Di Crescenzo, G., Santangelo, N., Santo, A., Valente, E., 2021. Geomorphological Approach to Cliff Instability in Volcanic Slopes: A Case Study from the Gulf of Naples (Southern Italy). Geosciences 11, 289.

Dickson, M.E., Ogawa, H., Kench, P.S., Hutchinson, A., 2013. Sea-cliff retreat and shore platform widening: steady-state equilibrium? Earth surface processes and landforms 38, 1046–1048.

Duperret, A., Genter, A., Mortimore, R.N., Delacourt, B., De Pomerai, M.R., 2002. Coastal rock cliff erosion by collapse at Puys, France: the role of impervious marl seams within chalk of NW Europe. Journal of Coastal Research , 52–61.

Earlie, C., Masselink, G., Russell, P., 2018. The role of beach morphology on coastal cliff erosion under extreme waves. Earth Surface Processes and Landforms 43, 1213–1228.

Emery, K., Kuhn, G., 1982. Sea cliffs: their processes, profiles, and classification. Geological Society of America Bulletin 93, 644–654.

Goda, Y., 2010. Random Seas and Design of Maritime Structures. volume 33. World Scientific Publishing Company.

Gornitz, V., White, T.W., Cushman, R.M., 1991. Vulnerability of the US to future sea level rise. Journal of Coastal Research 9, 201–237.

Gornitz, V.M., Daniels, R.C., White, T.W., Birdwell, K.R., 1994. The development of a coastal risk assessment database: vulnerability to sea-level rise in the US Southeast. Journal of Coastal Research 12, 327–338.

Hansom, J., Barltrop, N., Hall, A., 2008. Modelling the processes of cliff-top erosion and deposition under extreme storm waves. Marine Geology 253, 36–50.

Hapke, C., Plant, N., 2010. Predicting coastal cliff erosion using a bayesian probabilistic model. Marine Geology 278, 140–149.

Holthuijsen, L., Booij, N., Ris, R., 1993. A spectral wave model for the coastal zone, ASCE.

Johnstone, E., Raymond, J., Olsen, M.J., Driscoll, N., 2016. Morphological expressions of coastal cliff erosion processes in San Diego County. Journal of Coastal Research 76, 174–184.

Jones, D., Williams, A., 1991. Statistical analysis of factors influencing cliff erosion along a section of the West Wales coast, UK. Earth Surface Processes and Landforms 16, 95–111.

Jones, E.V., Rosser, N., Brain, M., Petley, D., 2015. Quantifying the environmental controls on erosion of a hard rock cliff. Marine Geology 363, 230–242.

Komar, P.D., Shih, S.M., 1993. Cliff erosion along the Oregon coast: A tectonic-sea level imprint plus local controls by beach processes. Journal of Coastal Research , 747–765.

Letortu, P., Jaud, M., Grandjean, P., Ammann, J., Costa, S., Maquaire, O., Davidson, R., Le Dantec, N., Delacourt, C., 2018. Examining high-resolution survey methods for monitoring cliff erosion at an operational scale. GIScience & Remote Sensing 55, 457–476.

Lim, M., Rosser, N.J., Petley, D.N., Keen, M., 2011. Quantifying the controls and influence of tide and wave impacts on coastal rock cliff erosion. Journal of Coastal Research 27, 46–56.

López-Ruiz, A., Bergillos, R.J., Lira-Loarca, A., Ortega-Sánchez, M., 2018a. A methodology for the long-term simulation and uncertainty analysis of the operational lifetime performance of wave energy converter arrays. Energy 153, 126–135.

López-Ruiz, A., Bergillos, R.J., Ortega-Sánchez, M., 2016a. The importance of wave climate forecasting on the decision-making process for nearshore wave energy exploitation. Applied energy 182, 191–203.

López-Ruiz, A., Bergillos, R.J., Ortega-Sánchez, M., Losada, M.A., 2016b. Impact of river regulation on the submerged morphology of a Mediterranean deltaic system: evaluating Coastal Engineering tools, in: Coastal Engineering Proceedings, p. 10.

López-Ruiz, A., Bergillos, R.J., Raffo-Caballero, J.M., Ortega-Sánchez, M., 2018b. Towards an optimum design of wave energy converter arrays through an integrated approach of life cycle performance and operational capacity. Applied Energy 209, 20–32.

Magaña, P., Bergillos, R.J., Del-Rosal-Salido, J., Reyes-Merlo, M.A., Díaz-Carrasco, P., Ortega-Sánchez, M., 2018. Integrating complex numerical approaches into a user-friendly application for the management of coastal environments. Science of the Total Environment 624, 979–990.

Moore, L.J., Griggs, G.B., 2002. Long-term cliff retreat and erosion hotspots along the central shores of the monterey bay national marine sanctuary. Marine Geology 181, 265–283.

Muñoz-López, P., Payo, A., Ellis, M.A., Criado-Aldeanueva, F., Jenkins, G.O., 2020. A method to extract measurable indicators of coastal cliff erosion from topographical cliff and beach profiles: Application to north norfolk and suffolk, east england, uk. Journal of Marine Science and Engineering 8, 20.

Ogawa, H., Dickson, M., Kench, P., 2011. Wave transformation on a subhorizontal shore platform, Tatapouri, North Island, New Zealand. Continental Shelf Research 31, 1409–1419.

Pappalardo, M., Cappietti, L., Llopis, I.A., Chelli, A., De Fabritiis, L., 2017. Development of shore platforms along the NW coast of Italy: The role of wind waves. Journal of Coastal Research 33, 1102–1112.

Prémaillon, M., Regard, V., Dewez, T.J., Auda, Y., 2018. GlobR2C2 (Global Recession Rates of Coastal Cliffs): a global relational database to investigate coastal rocky cliff erosion rate variations. Earth Surface Dynamics 6, 651.

del Río, L., Gracia, F.J., Benavente, J., 2016. Multiple-Source Cliff Erosion in Southern Spain: Current Risk and Future Perspectives. Journal of Coastal Research 75, 1072–1076.

Robinson, L., 1977. Marine erosive processes at the cliff foot. Marine Geology 23, 257–271.

Rodriguez-Delgado, C., Bergillos, R.J., 2021. Wave energy assessment under climate change through artificial intelligence. Science of The Total Environment 760, 144039.

Rodriguez-Delgado, C., Bergillos, R.J., Iglesias, G., 2019a. An artificial neural network model of coastal erosion mitigation through wave farms. Environmental Modelling and Software 119, 390–399.

Rodriguez-Delgado, C., Bergillos, R.J., Iglesias, G., 2019b. Dual wave energy converter farms and coastline dynamics: the role of inter-device spacing. Science of the Total Environment 646, 1241–1252.

Rodriguez-Delgado, C., Bergillos, R.J., Iglesias, G., 2019c. Dual wave farms for energy production and coastal protection under sea level rise. Journal of Cleaner Production 222, 364–372.

Rodriguez-Delgado, C., Bergillos, R.J., Iglesias, G., 2020. Coastal infrastructure operativity against flooding – a methodology. Science of The Total Environment 719, 137452.

Rodriguez-Delgado, C., Bergillos, R.J., Ortega-Sánchez, M., Iglesias, G., 2018a. Protection of gravel-dominated coasts through wave farms: Layout and shoreline evolution. Science of The Total Environment 636, 1541–1552.

Rodriguez-Delgado, C., Bergillos, R.J., Ortega-Sánchez, M., Iglesias, G., 2018b. Wave farm effects on the coast: The alongshore position. Science of the Total Environment 640, 1176–1186.

Rosser, N., Petley, D., Lim, M., Dunning, S., Allison, R., 2005. Terrestrial laser scanning for monitoring the process of hard rock coastal cliff erosion. Quarterly Journal of Engineering Geology and Hydrogeology 38, 363–375.

Sallenger Jr, A.H., Krabill, W., Brock, J., Swift, R., Manizade, S., Stockdon, H., 2002. Sea-cliff erosion as a function of beach changes and extreme wave runup during the 1997–1998 El Niño. Marine Geology 187, 279–297.

Shih, S.M., Komar, P.D., 1994. Sediments, beach morphology and sea cliff erosion within an oregon coast littoral cell. Journal of Coastal Research , 144–157.

Sunamura, T., 1977. A relationship between wave-induced cliff erosion and erosive force of waves. The Journal of Geology 85, 613–618.

Terefenko, P., Giza, A., Paprotny, D., Kubicki, A., Winowski, M., 2018. Cliff retreat induced by series of storms at Miedzyzdroje (Poland). Journal of Coastal Research , 181–185.

Terefenko, P., Paprotny, D., Giza, A., Morales-Nápoles, O., Kubicki, A., Walczakiewicz, S., 2019. Monitoring Cliff Erosion with LiDAR Surveys and Bayesian Network-based Data Analysis. Remote Sensing 11, 843.

Thierry, S., Dick, S., George, S., Benoit, L., Cyrille, P., 2019. EMODnet Bathymetry a compilation of bathymetric data in the European waters, in: OCEANS 2019-Marseille, IEEE. pp. 1–7.

Thompson, C.F., Young, A.P., Dickson, M.E., 2019. Wave impacts on coastal cliffs: Do bigger waves drive greater ground motion? Earth Surface Processes and Landforms 44, 2849–2860.

Veigas, M., López, M., Romillo, P., Carballo, R., Castro, A., Iglesias, G., 2015. A proposed wave farm on the Galician coast. Energy conversion and management 99, 102–111.

Westoby, M.J., Lim, M., Hogg, M., Pound, M.J., Dunlop, L., Woodward, J., 2018. Cost-effective erosion monitoring of coastal cliffs. Coastal Engineering 138, 152–164.

Zelaya Wziatek, D., Terefenko, P., Kurylczyk, A., 2019. Multi-Temporal Cliff Erosion Analysis Using Airborne Laser Scanning Surveys. Remote Sensing 11, 2666.